

Near field effect on horizontal equal-hazard spectrum of Tabriz city in north-west of Iran

J. Vafaie¹, T. Taghikhany^{2,*}, M. Tehranizadeh³

Received: August 2009, Revised: September 2010, Accepted: January 2011

Abstract

The near field ground motions have a high amplitude pulse like at the beginning of the seismogram which are significantly influenced by the rupture mechanism and direction of rupture propagation. This type of ground motion cause higher demands for engineering structures and its response spectrum is dramatically different than far field spectra. Tabriz is one of the ancient cities in Azerbaijan province with many industrial factories, financial centers and historical monuments in North-West of Iran. In this region, North Tabriz Fault which has a well known history of intense seismic activity is passing through in close distance of urban area. In this regard investigation of near field ground motion effect on current practice seismic design spectrum in this region is necessary. Hence, probabilistic seismic hazard analysis is carried out using appropriate attenuation relationship to consider near field effect. The peak ground acceleration (PGA) and several spectral accelerations (SA) over bedrock are estimated for different return periods and maps of iso acceleration contour lines are provided to indicate the earthquake hazard in different points of Tabriz city. Afterward, the generated horizontal equal-hazard spectrums considering near field effect are compared with different spectrums developed based on simple pulse model for near field motion. Both types spectrum are used for verifying current practice seismic design spectrum of Iranian code (2005) and International Building Code (IBC 2000). The results reveal the long-period structures which are seismically designed based on current practice seismic codes are in high risk of being damaged by attenuation relationships during near fault ground motion.

Keywords: Equal-Hazard Spectrum, Near Field Effect, Tabriz City.

1. Introduction

Failures of structures at urban area nearby seismic sources are significantly depended on rupture propagation of causative fault. Indeed, when the velocity of fault rupture toward a site is close to the shear wave velocity, the released seismic energy accumulates in a high amplitude pulse at the beginning of the record. This type of ground motion cause higher demands for engineering structures and its response spectrum is dramatically different from far field spectrum. Design spectrum in National Iranian Seismic Design Code does not provide an adequate representation of near fault ground motion [1,2] and any possible modification should be investigated for the urban area near to active seismic source.

Tabriz city in North-West of Iran is in region of intense deformation and seismicity, situated between two thrust belts of the Caucasus to the north and the Zagros Mountains to the south [3]. In this region, North Tabriz Fault which has a well known history of intense seismic activity is passing through in close distance of urban area. In order to investigate any possible modification of current practice seismic design code a probabilistic seismic hazard assessment is carried out considering near field phenomena in Tabriz region.

The earthquake catalogue in this study contains historical and instrumental events covering the period from the eighth century A.D to 2006. Eight potential seismic sources are modeled as area sources in a region between 45-47.5°E longitudes and 37-39°N latitudes. The PSHA is carried out for a grid of 81 points with 0.05° intervals in urban area and the maps have been prepared to indicate the earthquake hazard of city in the form of iso acceleration contour lines. The seismic hazard zoning maps are provided based on PGA and SA over seismic bedrock for %63, 10% and 2% probability of exceedance in 50 years for two attenuation relationships Bozorgnia&Campbell (2003) and

* Corresponding Author: ttaghikhany@aut.ac.ir

1 MS student, Department of Civil and Environmental Engineering, Amirkabir University of Technology, Tehran

2 Assistant Professor, Department of Civil and Environmental Engineering, Amirkabir University of Technology, Tehran

3 Professor, Department of Civil and Environmental Engineering, Amirkabir University of Technology, Tehran

Ambraseys&Douglas (2003).

These attenuation relations are used to estimate near field ground motion effect in probabilistic seismic hazard analysis.

Afterward, horizontal equal-hazard spectrums considering near field effect are generated for each of the 81 points in Tabriz zone and its average compared with different spectrums developed based on simple pulses model for near field motion. Both types spectrum used to verify design spectrum of Iranian Code of Practice for Seismic Design (2005) and International Building Code (IBC 2000).

2. Tectonic Setting

Tabriz region in northwestern of Iran as a part of the Alpine-Himalayan belt is in between the Arabian Shield in the south-west and the Eurasia plate in the north-east. Earthquake focal mechanisms indicate faults in region mainly are WNW-trending right-lateral strike-slip [4]. These strike-slip faults appear to be the southeastern continuation into North-West of Iran of the North Anatolian Fault and other right-lateral faults in sought-east of Turkey [3]. However, right-lateral faulting in the South-East of Turkey and North-West of Iran region is not continuous but consists of several discontinuous fault segments (Figures 1) [3].

The North Tabriz Fault is the most prominent tectonic structure in the immediate vicinity of Tabriz city with right-lateral fault mechanism. It has an average strike of NW-SE that is approximately N 115° E over a length of about 150 km, from Sufian city in the north-west to Bostanabad city in the south-east and appears to be generally close to vertical in dip. Among the many historical earthquakes that have occurred in the Tabriz region (e.g., the 858, 1042, 1273, 1304, 1550, 1641, 1717, 1721, 1780 and 1786 earthquakes), the destructive earthquakes of 1042 (Ms 7.3), 1721 (Ms 7.3) and 1780 (Ms 7.4) were accompanied by co-seismic surface faulting [3].

3. Source Zonation and Earthquake Database

Crustal faults and epicenter location of past earthquakes in the Tabriz region is shown in Figure 2 from the eighth century A.D. to 2006. The earthquake database has been prepared based on the available information from various sources like instrumental catalogues and the historical documents. The instrumental catalogues are USGS [5], IIEES [6], and the historical data is taken from published documents about history of Persian earthquakes [7].

Potential seismic source regions in Figure 2b are chosen mainly based on tectonic information, epicenter distributions of earthquakes and available geological and geophysical information. Twenty active faults considered in study region, viz. North Tabriz fault, the Mishu fault, the Sharafkhaneh-Sofian fault, etc. are allocated to six areas source as shown in figure.

4. Maximum Magnitude Determination

Selection of a maximum magnitude for each source is ultimately a judgment that incorporates understanding of specific fault characteristics, the regional tectonic environment, and data on regional seismicity. For the purpose of seismic hazard modeling, the maximum earthquake magnitude for each of the seismic sources is determined by the fault rupture length procedure. In this method the empirical relationships used for determining maximum magnitude earthquake of seismic source zone based on rupture length. Many available seismological data of earthquakes in Iran are used in empirical relationship suggested by Nowroozi (1976) [8]. His suggested relationship is used in this study as:

$$M_s = 1.259 + 1.244 \log L \quad (1)$$

Where, L is the surface rupture length in km.

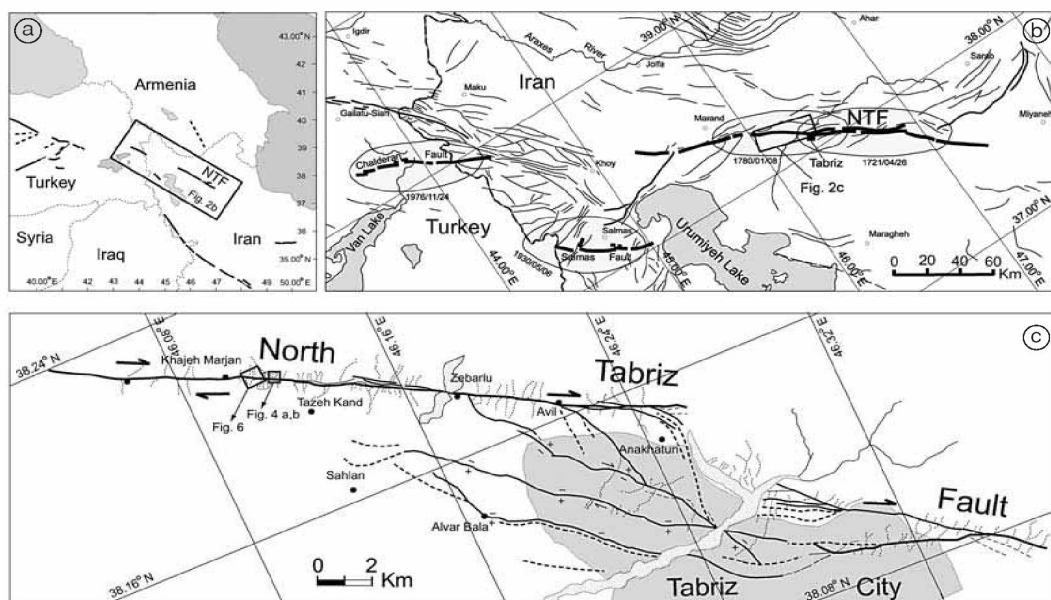


Fig. 1. a) Small-scale regional map of active faults in Northwestern Iran-Eastern Turkey. b) Simplified map of the North Tabriz fault. c) Northwestern section of the North Tabriz Fault [3].

5. Evaluation Earthquake Recurrence

In order to evaluate seismicity of region, the available data from past earthquakes is used in computation of the regression constants to accomplish the method of Gutenberg and Richter [9]. In Gutenberg and Richter recurrence relationship (Eq.2) the classical description of seismic activity is based on seismic activity rate, (α), which is equal to the number of events with magnitudes equal or greater than a defined magnitude level, during specific time period, T and on source area A; the parameter β ; the linear segment is bounded by a maximum magnitude determined as discussed above and by a minimum magnitude below which the data becomes incomplete and not of interest. $N(m)$ is the average number of events equal to or greater than magnitude m .

$$\ln N(m) = \alpha - \beta m \quad (2)$$

Herein, seismicity parameters could not be determined reliably for all area sources that were small or had incomplete seismic histories. Thus, recurrence relationship acquired based on available data across the region as following equation and normalized for each area source:

$$\ln N(m) = 11.82 - 1.70m \quad (3)$$

6. Near Field Effects and Appropriate Attenuation Relationship

Near field ground motions are affected by direction of rupture propagation to site (forward directivity effect) and residual displacement due to tectonic deformation (fling-step effect). Forward directivity occurs because the propagation velocity of fault rupture toward a site is close to the shear wave velocity. Fling-step waveforms are characterized by offset displacements in the slip-parallel direction, and large, unidirectional velocity pulses [10,11].

Since the attenuation relationships highly influence the

results of seismic hazard analysis, the choice of the ground motion attenuation that is identified based on the strong ground motion in vicinity of rupture area is of great importance. In the past because of a lack of adequate strong-motion data for large magnitude earthquakes from vicinity of focal center, equations to estimate strong ground motions have been derived mainly using strong-motion records from the intermediate- and far-field of earthquakes. However at the present sufficient strong-motion records for large magnitude earthquakes from vicinity of focal center have become available to derive equations for estimating ground motions using such records, attenuation relationships suffer from lack of sufficient accuracy [12].

Two selected worldwide attenuation, Ambraseys&Douglas (2003) [12] and Bozorgnia&Campbell (2003) [13], not only identified based on the seismic motion close to rupture area in whole of the world; but also they used some records of earthquakes that took place in Iran.

Ambraseys & Douglas selected 186 free-fields, chiefly triaxial strong-motion records from 42 earthquakes. Their attenuation relationship is [12]:

$$\log y = b_1 + b_2 M_s + b_3 d + b_4 S_A + b_5 S_S \quad (4)$$

Where M_s is the surface-wave magnitude, S_A and S_S were taken the value of 0 because the site classified as rock.. The distance dependence defined in terms of $r = \sqrt{d^2 + h^2}$ in which d is the closest distance to the surface projection of the rupture, and h is source depth. Peak Ground Acceleration or Spectral Accelerations is termed as y which can be computed for a verity of parameters (b_1, b_2, b_3, b_4, b_5).

The second attenuation relationship is developed as a world average by Bozorgnia&Campbell (2003) [13]:

$$\ln Y = c_1 + f_1(M_w) + c_4 \ln \sqrt{f_2(M_w, r_{seis}, S)} + f_3(F) + f_4(S) + f_5(HW, F, M_w, r_{seis}) + \varepsilon \quad (5)$$

Where $f_1(M_w)$ is the magnitude scaling characteristic,

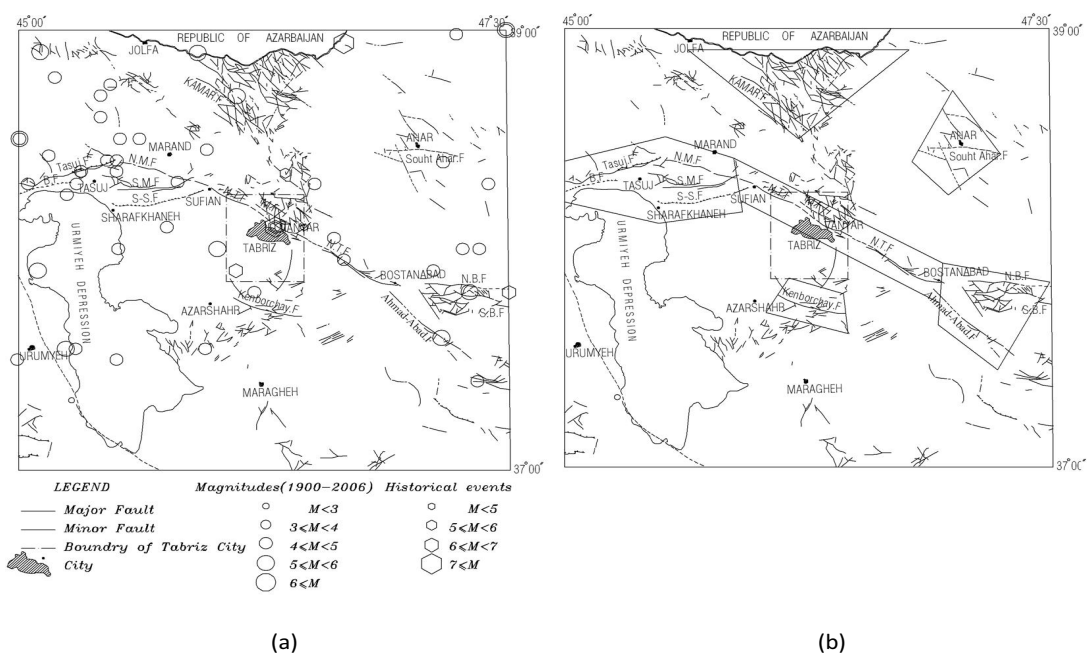


Fig. 2. a) Map of tectonic elements and seismicity in the Tabriz region. b) Potential area sources selected for seismic hazard assessment.

($f_1(M_w)=c_2M_w+c_3(8.5-M_w)^2$), $f_2(M_w, r_{seis}, S)$ is the distance scaling characteristic, ($f_2(M_w, r_{seis}, S)=r_{seis}^2+g(S)2(\exp[c_8M_w+c_9(8.5-M_w)^2])^2$ and $g(S)=c_5+c_6(S_{VFS}+S_{SR})+c_7S_{FR}$), $f_3(F)$ is the effect of faulting mechanism, ($f_3(F)=C_{10}F_{RV}+c_{11}F_{TH}$), $f_3(S)$ is the far-source effect of local site condition, ($f_4(S)=c_{12}S_{VFS}+c_{13}S_{SR}+c_{14}S_{FR}$), $f_5(HW, F, M_w, r_{seis})$ is the effect of the hanging wall, $f_5(HW, F, M_w, r_{seis})=HWf_3(F)f_{HW}(M_w)f_{HW}(r_{seis})$. closest fault to study area is the North Tabriz Fault, ($r_{jb} \leq 5km$), and its rupture surface slip is approximately vertical, ($\delta \simeq 90^\circ$), so there are $HW=0$ for $r_{jb} \geq 5km$ or $\delta > 70^\circ$, $S_{SR}=1$ for soft rock and $F_{RV}=F_{TH}=0$ for strike-slip and normal faulting.

They uniformly defined the size of an earthquake in terms of M_w and defined the source-to-site distance in terms of r_{seis} , the shortest distance between the recording site and the zone of the seismogenic energy release on the causative fault, referred to as the distance to seismogenic rupture [13]. The strong-motion parameters included in the analysis are peak ground acceleration and 5%-damped acceleration response spectrum (S_A) at natural periods ranging from 0.05 to 4.0 seconds. The moment magnitude (M_w) is defined as:

$$M_w = (2/3) \log M_0 - 10.7 \quad (6)$$

The seismic moment, M_0 that is described as [14]:

$$M_0 = 1.25 M_S + 17.83 \quad (7)$$

7. Probabilistic Seismic Hazard Analysis

The methodology used to conduct Probabilistic Seismic Hazard Analysis (PSHA) was initially developed by Allen Cornell in 1968 [15]. PSHA integrates over all possible earthquake ground motions at a site to develop a composite representation of the spectral amplitudes and hazards at that site. Application of the procedure includes several steps. The initial step requires the definition of potential seismic sources, usually associated with geological or tectonic features. In the next step, seismicity parameters are determined for each source zone. The distribution of earthquakes is described by a Poisson process and that earthquake magnitudes follow a Gutenberg-Richter doubly truncated distribution. The final step requires the integration

of individual contributions from each source zone into a site-specific distribution [16].

In this study, provided program by authors in Matlab software [17] is used to compute Peak Ground Acceleration (PGA) and Spectral Acceleration (S_A) parameters according the above mentioned procedure. The hazard curves for a grid of 81 points across Tabriz city are developed at ten selected periods of vibration for two different attenuation relationships.

The results are presented in Figures 3 and 4 as seismic zoning maps of the Tabriz region for 2% and 10% probability of exceedance (return period of 2475 years and 475 years) with using two attenuation relationships, Bozorgnia&Campbell (2003) and Ambraseys&Douglas (2003).

Acceleration contour lines in these figures are in good agreement with North Tabriz Fault trend and their values are in inverse proportion to distance from fault line. In these maps, for 10% probability of exceedance in 50 years, PGA are ranged between 0.2g to 0.65g for Bozorgnia&Campbell equation and varies between 0.2g to 0.55g for Ambraseys&Douglas relationship.

The PGA recommended in Iranian Code of Practice for Seismic Design in this region is equal to 0.35g. As it shown this value in some parts which are closer to North Tabriz Fault is less than 60 percent of estimated acceleration. These figures display PGA for 2% probability of exceedance in 50 years that are between 0.3g to 0.9g for both attenuation relationships.

8. Horizontal Equal-Hazard Spectrum

The approaches that can be followed in specifying site-specific spectrum on the basis of a probabilistic seismic hazard analysis involve anchoring a spectral shape to a peak acceleration level determined from a PSHA for peak acceleration or estimating the entire spectrum on the basis of PSHA for response spectral values at a number of periods of vibration that is called an horizontal equal-hazard spectrum [16]. The equal-hazard spectrum is developed from hazard curves for peak ground acceleration (PGA) and response spectral amplitudes (SA) at different periods of

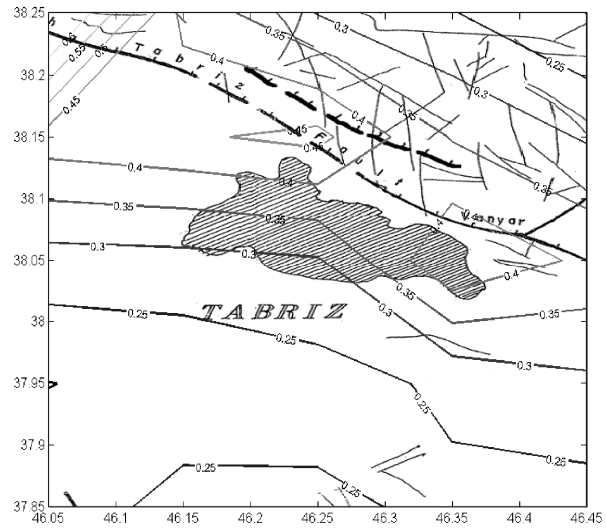
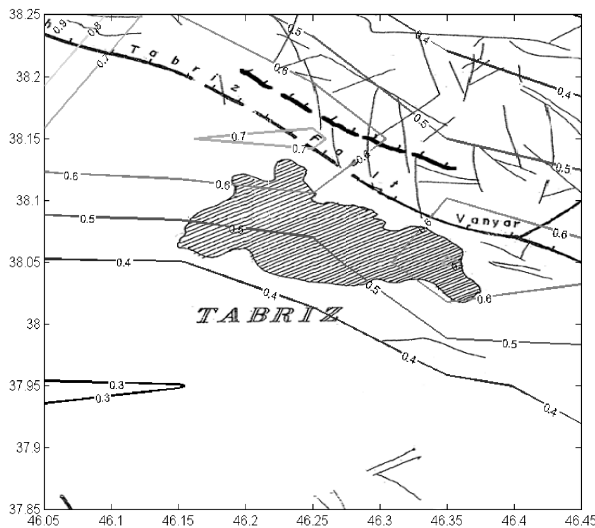


Fig. 3. Maps of iso acceleration contour lines (g) in Tabriz region for 2% (left) and 10% (right) probability of exceedance in 50 years, using Bozorgnia&Campbell (2003)

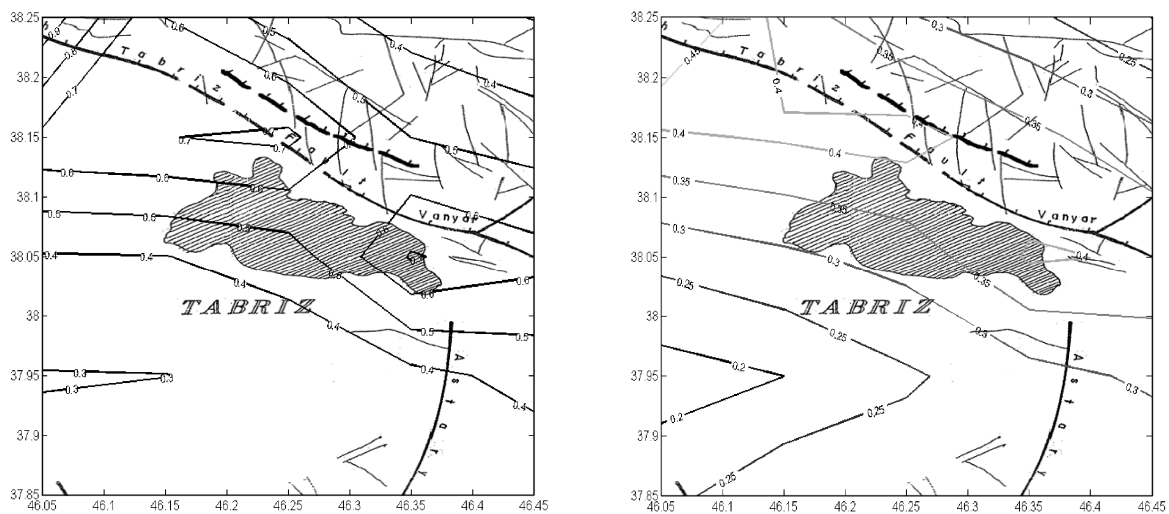


Fig. 4. Maps of iso acceleration contour lines (g) in Tabriz region for 2% (left) and 10% (right) probability of exceedance in 50 years, using Ambraseys&Douglas (2003)

vibration (T).

Herein, in order to appraise seismic response of structures in close distance of North-Tabriz Fault, the equal-hazard spectrums are constructed for 81 grid points in Tabriz boundary for %2, %10 and 63% probability of exceedance in 50 years. The acceleration response spectrums (SA) are computed at natural periods ranging from 0.1 to 2.0 seconds (0.10, 0.15, 0.20, 0.30, 0.40, 0.50, 0.75, 1.00, 1.50, and 2.00 seconds) for two attenuation relationships.

In order to recognize near field effect on seismic design spectra in region two equal-hazard spectrums in one and ten kilometers of Tabriz Fault are presented in Figure 5 and 6.

Figure 5 shows the results of PSHA's for peak ground acceleration and 5 percent-damped spectral ordinates at ten selected periods of vibration for two sites in one and ten kilometers distance of North-Tabriz Fault with three different hazard level for Bozorgnia&Campbell (2003) attenuation relationship. Figure 6 shows these equal-hazard spectrums for Ambraseys&Douglas (2003) attenuation relationship.

Comparing generated horizontal equal-hazard spectrums in one and ten kilometer distance from North-Tabriz shows near field ground motion considerably amplify seismic response of medium and long period structures.

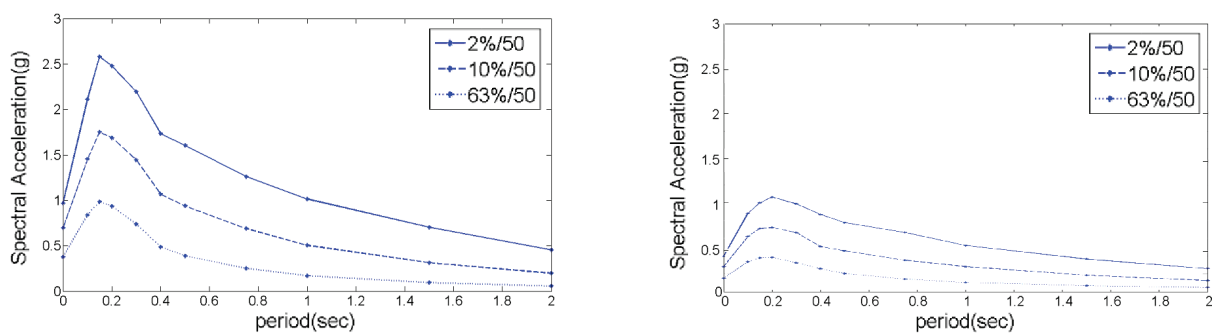


Fig. 5. Horizontal equal-hazard spectrum for site in one (left) and ten (right) kilometers distance of North-Tabriz Fault for %2, %10 and %63 probability of exceedance in 50 years using the attenuation relationship of Bozorgnia&Campbell (2003).

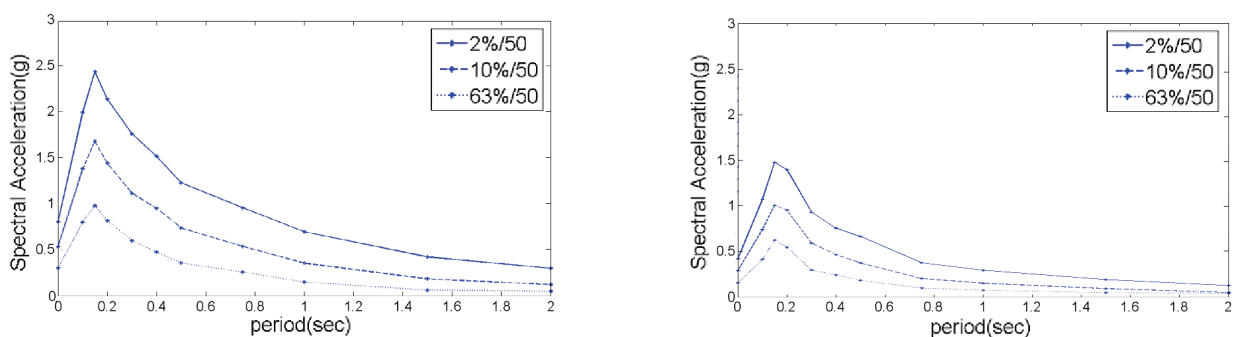


Fig. 6. Horizontal equal-hazard spectrum for site in one (left) and ten (right) kilometers distance of North-Tabriz Fault for %2, %10 and %63 probability of exceedance in 50 years using the attenuation relationship of Ambraseys&Douglas (2003).

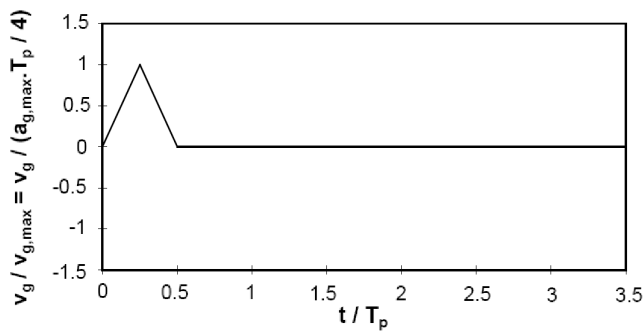


Fig. 7. The half-pulse shape that is utilized to model the simple near field pulses [10]

9. Near Field Pulse Model Spectrum

High amplitude pulse like at the beginning of the seismogram in near field ground motions can be modeled by simple pulse motion. Studies by researchers, such as Krawinkler and Alavi [10] and Somerville et al [18], have shown that simplified representations of the velocity pulse are capable of capturing the salient response features of structures subjected to near-fault ground motions. The simplified sine-pulse representations of velocity-time histories are defined by the number of equivalent half-cycles of pulse motion, the period of each half-cycle, and their corresponding amplitudes.

Half pulse model introduced by Alavi & Krawinkler are fully defined by pulse shape that shown in Figure 7 and two parameters, the pulse period and a pulse velocity. They have

developed a relationship between the period of the pulse of the near-fault (T_p) and the moment magnitude (M_w). In addition they made a relationship between the pulse effective velocity, the moment magnitude (M_w) and closest distance (R) [10].

$$\log T_p = -2.06 + 0.34M_w \quad (8)$$

$$\log V_{eff} = -4.04 + 0.88M_w + 0.2\log R \quad (9)$$

On the other hand, Somerville et al [18] have developed a model that relates the period of the pulse and peak ground velocity of ground motion to the moment magnitude (M_w) and closest distance (R) as follow:

$$\log T_p = -3.1 + 0.5M_w \quad (10)$$

$$\log PGV = -1.0 + 0.5M_w - 0.5\log 10R \quad (11)$$

These pulse velocity motions are used to develop 5 percent-damped response spectrums to verify the produced equal hazard spectrum in region. In Eq.9 and Eq.10, M_w are assumed 7.62, 7.35 and 6.7 Richter scale for 2, 10 and 63 percent probability of exceedance in 50 years respectively. Gutenberg and Richter recurrence relationship in Eq.2 have been used for computing above magnitude for different hazard levels.

Figures 8 and 9 show two spectrums for one and ten kilometers distance according to Alavi & Krawinkler and Somerville et al. equations respectively. In both figures, near field effect amplify spectral acceleration in velocity region of both spectrums.

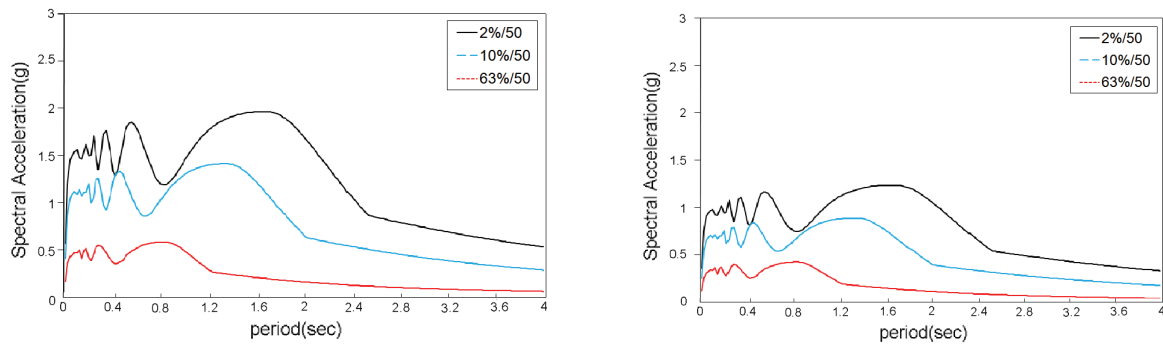


Fig. 8. Pulse model spectrum for 5 percent-damping according to Alavi & Krawinkler relationship in one (left) and ten (right) kilometers distance from Tabriz fault for %2 , %10 and %63 probability of exceedance in 50 years.

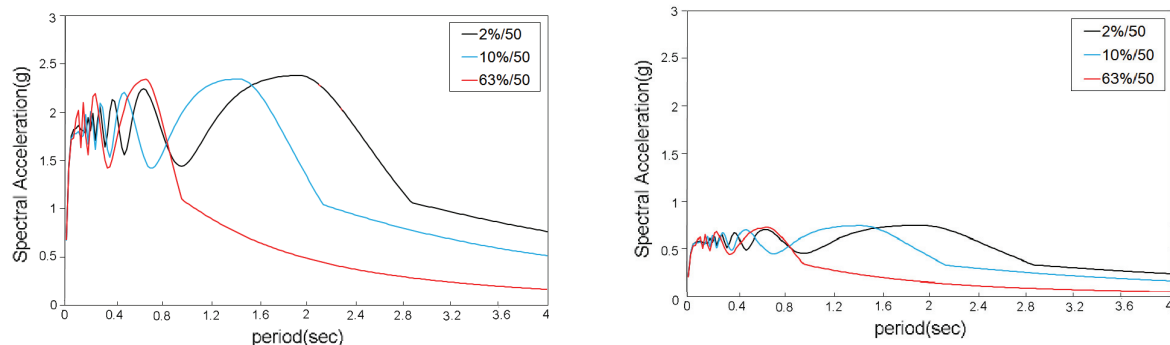


Fig. 9. Pulse model spectrum for 5 percent-damping according Somerville et al relationship in one (left) and ten (right) kilometers distance from Tabriz fault for %2 , %10 and %63 probability of exceedance in 50 years.

10. Comparison of Equal Hazard and Standard Spectrums

Here, average equal hazard spectrums of both attenuation relationships are computed for two different sites in one and ten kilometers distance from North-Tabriz Fault. Its results are compared with average simple pulses spectrum according Alavi & Krawinkler and Somerville et al. equations. These spectrums for %10 probability of exceedance in 50 years are shown in Figure 10. In velocity region, average simple pulses spectrums are shown higher spectral acceleration than average equal hazard spectrums.

In addition, the average equal hazard spectrums for the sites at one and ten kilometers of North-Tabriz Fault for %10 probability of exceedance in 50 years are compared with design spectrum of Iranian Code of Practice for Seismic Design (2005) and International Building Code (IBC 2000) for stiff soil in Figures 11. As it shown in figure, at one kilometers of North-Tabriz Fault the equal hazard spectrums in acceleration region (short period) are more close to design spectrum of International Building Code (IBC 2000) than recommended spectrum by Iranian Code of Practice for Seismic Resistant Design of Buildings. However, the simple pulse spectrum for site at one kilometer distance from North-Tabriz Fault has higher values than two design code spectrums at different periods.

Average spectrum for site in the 10 kilometers of North-Tabriz Fault has the same dynamic amplification of the IBC 2000.

11. Conclusion

In order to calculate seismic hazard in probabilistic process for the Tabriz region, a grid of 81 points with 0.05o intervals in urban area involved the 46.05-46.45oE longitudes and 37.85-38.25oN latitudes determined. For study in this urban area in near field the study area encompassed by the 45-47.5oE longitudes and 37-39oN latitudes. 10 active faults in Tabriz region in about 150-km distance indentified. PGA, SA values and equal-hazard spectrums have been computed for each grid points. The final results of the study are 66 iso-acceleration maps for %63 probability of exceedance in 50 years (return period of 72 years) and %10 probability of exceedance in 50 years (return period of 475 years) and %2 probability of exceedance in 50 years (return period of 2475 years) for two attenuation relationship of Bozorgnia & Campbell (2003) and Ambraseys & Douglas (2003) and for eleven selected periods of vibration (PGA, 0.10, 0.15, 0.20, 0.30, 0.40, 0.50, 0.75, 1.00, 1.50 and 2.00 seconds). Note that 50 years is the lifetime of the structures to be designed in the site. Only four of these iso-acceleration maps about PGA with return periods of 2475 and 475 years are presented in this article. Based on these values, 81 Equal-hazard spectrums have been designed for each grid point of Tabriz urban area. We use these iso-acceleration maps to create an equal-hazard spectrum for a specific site in Tabriz urban area. The results show a good agreement with North Tabriz Fault of the region. This fault is in vicinity of the Tabriz urban area and it is most active fault in the study region. According to the obtained results, PGA values are evaluated to be between 0.2g to 0.65g for the 475 years and 0.3g to 0.9g

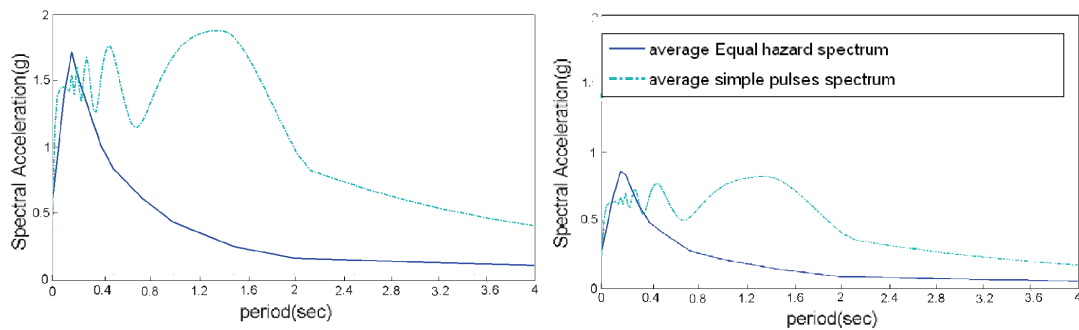


Fig. 10. Average pulse model spectrum are compared to equal hazard spectrum in the sites at one (left) and ten (right) kilometers of North-Tabriz Fault, for %10 probability of exceedance in 50 years

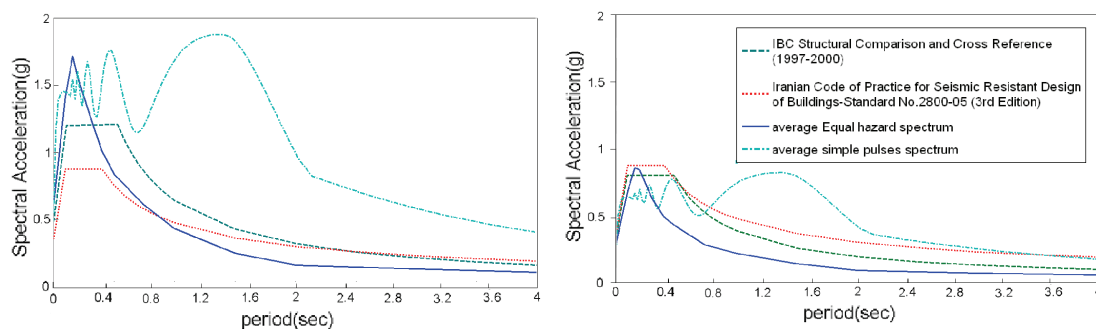


Fig. 11. Comparison of simple pulse model and equal hazard spectrum with Standard Spectrums at one (in left) and ten (in right) kilometer of North-Tabriz Fault , for %10 probability of exceedance in 50 years

for 2475 years return period for attenuation relationship of Bozorgnia&Campbell (2003) and they are evaluated to be between 0.2g to 0.55g for 475 years and 0.3g to 0.9g for 2475 years return period for attenuation relationship of Ambraseys&Douglas (2003).

References

- [1] Ghodrati Amiri G., Manouchehri Dana F., Sedighi S., "Determination of Design Acceleration Spectra for Different Site Conditions, Magnitudes, Safety Levels and Damping Ratios in Iran". (2008) International Journal of Civil Engineering; 6 (3) :184-181
- [2] Ghodrati Amiri G., Asadi A., "Comparison of Different Methods of Wavelet and Wavelet Packet Transform in Processing Ground Motion Records". (2009). International Journal of Civil Engineering; 7 (4) :248-257
- [3] Hessami, K. Pantosti, D. Tabassi, H. Shabani, E. Abbassi, M. Feghhi, K. Solaymani, S. 2003. "Paleoearthquakes and Slip Rates of the North-Tabriz Fault, NW Iran: Preliminary Results" Annals of Geophysics, Vol. 46, N. 5.
- [4] JACKSON, J. 1992. "Partitioning of Strike-Slip and Convergent Motion between Eurasia and Arabia in Eastern Turkey and the Caucasus". J. Geophys. Res., 97, 12471-12479.
- [5] U.S. Geological Survey (USGS), <http://www.usgs.gov/>
- [6] International Institute of Earthquake Engineering and Seismology (IIEES), <http://www.iiees.ac.ir>
- [7] Ambraseys, N.N. Melville, C. P. 1982. "A History of Persian Earthquakes". Cambridge University Press.
- [8] Nowroozi, A.A. 1976. "Siesmotectonic Provinces of Iran," Bull. Seism. Soc. Am, Vol. 66, No. 4.
- [9] Gutenberg, B. and Richter, C. F. 1954. "Seismicity of the Earth and Associated Phenomena", Princeton Univ. Press, Princeton, New Jersey, U.S.A.
- [10] Alavi, B. and Krawinkler, H. 2001. "Effects of Near-Fault Ground Motions on Frame Structures". Ph.D. Department of Civil and Environmental Engineering Stanford University, California. USA.
- [11] Stewart, JP. Chiou, SJ. Bray, JD. Graves, RW. Somerville, PG. Abrahamson, NA. 2002. "Ground Motion Evaluation Procedures for Performance-Based Design". J. Soil Dynamics and Earthquake Engineering, Vol 22. PP 765-772.
- [12] Ambraseys, N.N., Douglas, J. 2003. "Near-Field Horizontal and Vertical Earthquake Ground Motions", J. Soil Dynamics and Earthquake Engineering, 23, 1-18
- [13] Bozorgnia, Y. Campbell, K. W. 2003. "The Vertical-to-Horizontal Response Spectrum Ratio and Tentative Procedures for Developing Simplified V/H and Vertical Design Spectrum" J. Earthquake Engineering, Vol. 8, No. 2. P.175-207.
- [14] Wang, J, H. 1992. "Magnitude Scales and Their Relations for Taiwan Earthquakes". TAO, vol3, no.4. 449-468
- [15] Cornell, C.A. (1968). "Engineering seismic risk analysis, Bull. Seism. Soc." Am., 58, 1583-1606.
- [16] Manual No. 1110-2-6050, 1999. "Response Spectrum and Seismic Analysis for Concrete Hydraulic Structures". Department of the Army U.S. Army Corps of Engineers.
- [17] MathWorks. 2006. MATLAB User's Guide.
- [18] Somerville, P.G., K. Irikura, R. Graves, S. Sawada, D. Wald, N. Abrahamson, Y. Iwasaki, T. Kagawa, N. Smith and A. Kowada (1998). "Characterizing Earthquake Slip Models for the Prediction of Strong Ground Motion". Seismological Research Letters, 70, 59-80.